Histol Histopathol (2024) 39: 1359-1370

Histology and Histopathology
From Cell Biology to Tissue Engineering

ORIGINAL ARTICLE Open Access

Upregulation of LY6K induced by FTO-mediated demethylation promotes the tumorigenesis and metastasis of oral squamous cell carcinoma via CAV-1-mediated ERK1/2 signaling activation

Chen Xu, Rujuan Gong and Haibing Yang

Department of Stomatology, Changzhou Second People's Hospital, Changzhou, Jiangsu Province, China

Summary. Lymphocyte antigen 6 complex locus K (LY6K) has been demonstrated to play a significant role in cancers and identified as a therapeutic biomarker for head and neck squamous cell carcinoma. However, the role of LY6K in oral squamous cell carcinoma (OSCC) has not been explored. The current study discovered that LY6K was aberrantly upregulated in OSCC cell lines and tissues and that high LY6K expression significantly correlated with poorer survival of OSCC patients. Through stable knockdown of LY6K, we found that the growth, colony formation, migration, and invasion of OSCC cells were substantially suppressed. In addition, tumor growth and lung metastasis *in vivo* were effectively inhibited by LY6K depletion. Mechanically, LY6K binds with CAV-1 and activates CAV-1-mediated MAPK/ERK signaling to exert its oncogenic effects on OSCC. In addition, LY6K expression in OSCC was discovered to be regulated by FTO-mediated RNA N6-methyladenosine (m^6A) modification in an IGF2BP1-dependent manner. Generally, LY6K expression was upregulated by FTO-mediated demethylation in OSCC, which promoted the tumorigenesis and metastasis of OSCC via activating the CAV-1-mediated ERK1/2 signaling pathway.

Key words: Oral squamous cell carcinoma, LY6K, FTO, m^6A modification

Corresponding Author: Rujuan Gong, Department of Stomatology, Changzhou Second People's Hospital, No. 29 Xinglong Lane, Tianning District, Changzhou City, Jiangsu Province, 213000, China. e-mail: xu_chen233@126.com

www.hh.um.es. DOI: 10.14670/HH-18-725

Introduction

Oral cancer, specifically oral squamous cell carcinoma (OSCC), is a prevalent type of cancer worldwide, with over 300,000 new cases each year (Arellano-Garcia et al., 2010). Tobacco smoking and alcohol consumption are significant risk factors for developing OSCC (Keinänen et al., 2021). OSCC often originates from pre-existing oral lesions known as oral potentially malignant disorders, which pose an increased risk of cancer progression (Wang and Wang, 2021). Despite improvement in treatment therapies, the overall survival of late-stage OSCC remains pessimistic (Yang et al., 2019). The unfavorable prognosis of OSCC is associated with certain factors, such as delayed diagnosis, shorter time recurrences, positive margin status, lymphovascular invasion, and higher histopathological grading, and early detection can improve the prognosis for OSCC patients (Vitório et al., 2020).

Lymphocyte antigen 6 complex locus K (LY6K), a member of the Ly6/urokinase-type plasminogen activator receptor family (Kim et al., 2016), is expressed in testicular cells and assists fertilization by facilitating the migration of spermatozoa toward the oviduct (Fujihara et al., 2018). LY6K is also expressed in human cancer cells and is one of the cancer/testis antigens (CTA) (Kono et al., 2009). Since CTAs have cancer-restricted expression and immunogenic properties, they are considered ideal for targeted immunotherapy (Caballero and Chen, 2012). Noticeably, LY6K was identified as a potential target for head and neck squamous cell carcinoma by multiple studies (de Nooij-van Dalen et al., 2003; Carrero et al., 2019). Currently, there has been no detailed report on the biological function of LY6K in OSCC.

In addition, DNA methylation was reported to regulate LY6K expression in glioblastoma, and irradiation induces LY6K upregulation by promoter demethylation, resulting in enhanced radiation resistance

in glioma stem-like cells (Sastry et al., 2020). In breast cancer, inhibition of DNA methylation with 5-Aza-dC caused elevated LY6K expression, resulting in enhanced cell migration ability (Kong et al., 2014). Regarding its downstream mechanism, studies have suggested that LY6K binds with caveolin-1 (CAV-1) and activates MAPK/ERK signaling (Sastry et al., 2020; Park et al., 2023). Nevertheless, the molecular mechanism of LY6K in OSCC has not been reported.

The current study was designed on the basis that m^6A modification-mediated upregulation of LY6K promoted tumorigenesis and metastasis in OSCC by activating CAV-1-regulated MAPK/ERK signaling. Our study may identify LY6K as a novel therapeutic biomarker in OSCC and elucidate the underlying mechanism involved, providing insights for OSCC diagnosis and treatment.

Materials and methods

Tissue samples

A total of 70 pairs of OSCC and adjacent normal tissues (>2 cm from the edge of OSCC tissues) were collected at Changzhou Second People's Hospital and put into liquid nitrogen for storage immediately after resection. Informed consent was obtained from all patients, and the study protocols were approved by the Ethics Committee of Changzhou Second People's Hospital.

Cell lines

Five OSCC cell lines including SCC9, SCC25, CAL27, HN4, and human oral keratinocyte (HOK) cells were purchased from ATCC (Manassas, VA, USA), and cultured in Dulbecco's Modified Eagle Medium (DMEM) with 10% fetal bovine serum (FBS), 100 U/ml penicillin and 0.1 mg/ml streptomycin.

Cell transfection

Short hairpin RNA targeting LY6K (shLY6K), FTO (shFTO), IGF2BP1 (shIGF2BP1), CAV-1 (shCAV-1), and negative control (shNC); overexpression plasmid containing LY6K (oeLY6K) and empty pcDNA3.1 vector as control (oeNC) were all synthesized and provided by GenePharma (Shanghai, China). These vectors were transfected into CAL27 and HN4 cells using Lipofectamine 2000 and subjected to experiments 48 hours following transfection.

RT-qPCR

Total RNA extraction was performed using TRIzol reagent (Invitrogen, USA), and reverse transcribed into cDNA using the One Step TB Green® PrimeScript™ RT-PCR Kit (Takara, Japan) and then quantified with specific primers on the Applied Biosystems 7300 Real-Time PCR System (ThermoFisher). GAPDH mRNA was employed as a control, and the $2^{-\Delta\Delta Ct}$ formula was used to calculate relative gene levels.

Co-immunoprecipitation (Co-IP) assay

Cells were lysed in RIPA lysis buffer containing protease and phosphatase inhibitor cocktails (Sigma-Aldrich). Then, cell lysates were pre-cleared with 50 µl Protein A agarose bead slurry per 1 mg lysate for 1 hour at 4°C on a rotator, followed by centrifugation at 1,000 rpm for 3 min at 4°C, and immunoprecipitation with LY6K antibody for 12 hours overnight at 4°C.

RNA immunoprecipitation (RIP) assay

RIP assays were performed using an EZ-Magna RIPTM RNA-Binding Protein Immunoprecipitation Kit (Millipore Sigma, cat. 17-700). Briefly, cell supernatants were lysed with radioimmunoprecipitation assay lysis buffer containing an RNase inhibitor and proteases, and then incubated with IGF2BP1 antibody beads overnight at 4°C. Proteinase K (Millipore Sigma, cat. 71049) was added, and the mixture was incubated at 65°C for 30 min with occasional shaking of the beads. Finally, total RNA was isolated using TRIzol reagent and subjected to qPCR.

Western blot

Total protein was isolated by RIPA buffer. After quantification using the BCA Protein Quantification Kit (ThermoFisher), 10 µg of protein was loaded onto an SDS-PAGE gel for separation. Subsequently, the protein signal was transferred onto a PVDF membrane and blocked with 5% non-fat milk powder. The membrane was incubated with primary antibodies against LY6K, FTO, CAV-1, ERK, phosphorylated (p)-ERK, and GAPDH overnight at 4°C. After incubating with the appropriate secondary antibody at 37°C for 1h, the blot was visualized using the ECL detection system (ThermoFisher).

CCK-8 and colony formation assays

For the CCK-8 assay, OSCC cells were plated in 96-well plates and then cultured for 3 days following treatment with 10 µl CCK-8 reagent (Dojindo, Japan). The absorbance at 450 nm reflected cell viability. For colony formation assay, cells were seeded in 6-well plates and cultured for 2 weeks. Then, cells were stained with crystal violet.

Cell migration and invasion assays

Transwell chambers with or without Matrigel coating were used to assess cell invasion and migration, respectively. In short, cells suspended in FBS-free DMEM/F12 culture medium were added into the upper

chamber, and the lower chamber was filled with 1 mL of DMEM/F12 containing 10% FBS as a chemo-attractant. After incubation for 24h, the cells adhered to the lower membrane surface were stained with 0.1% crystal violet. Images were captured and the stained cells were quantified under a microscope from five random fields.

Xenograft mouse model

Mice aged 4-6 weeks were purchased from the Shanghai Experimental Animal Center, Chinese Academy of Sciences (Shanghai, China), and randomly divided into two groups (n=3/group). LY6K-silenced CAL27 cells were injected subcutaneously into mice. After five weeks, all mice were sacrificed and tumor tissues were weighed and photographed. For the lung metastasis assay, stably infected CAL27 cells were injected into the tail vein of BALB/c nude mice. After six weeks, the mice were sacrificed, and the lungs were embedded, sectioned, and stained with H&E to reveal the number of metastatic nodules.

Luciferase reporter assay

LY6K 3'-UTR containing predicted m^6A motifs were synthesized and inserted into the pmirGLO vector (Promega, Madison, WI, USA), followed by transfection into control and FTO-silenced cells using Lipofectamine 2000 (Invitrogen). The adenine to guanine mutation was conducted by TaKaRa MutanBEST Kit (TaKaRa) as per the supplier's instructions. Luciferase activity was detected using the Dual-Luciferase® Reporter Assay System (Promega).

Methylated RNA immunoprecipitation (MeRIP) assay

The MeRIP assay was conducted using the Magna MeRIP m^6A Kit (Millipore, Germany). In brief, total RNA was extracted using the miRNeasy Mini Kit (Qiagen, Dusseldorf, Germany) with stringent DNA digestion, followed by chemical fragmentation to about 100 nt. RNA was then immunoprecipitated with 5 µg m^6A antibody or anti-mouse IgG linked to protein A/G magnetic beads. After elution, m^6A enrichment on LY6K mRNA 3'-UTR was analyzed by qRT-PCR, normalizing to input (10% fragmented RNA).

Statistical analysis

All data were analyzed using SPSS version 22 (SPSS Inc., Chicago, IL, USA) and figures were generated using GraphPad Prism 8 software and shown as mean ± standard deviation (SD) of at least three independent experiments carried out in triplicate. The correlation between LY6K levels and OSCC survival times was determined by the Kaplan-Meier plotter. Student's t-test was used to assess the difference between the two groups. A P-value <0.05 was considered statistically significant.

Results

LY6K expression is upregulated in OSCC

As indicated by GEO datasets, LY6K expression was higher in OSCC tissues and cell lines than that in non-tumor tissue and cells (Fig. 1A,B). To verify, we compared the LY6K mRNA and protein levels in OSCC cell lines (SCC9, SCC25, CAL27, and HN4) and HOK cells. As shown in Fig. 1C,D, the LY6K level was significantly elevated in all OSCC cell lines compared with HOK cells. Consistently, LY6K was abundantly expressed in OSCC tissues in comparison with adjacent normal tissues (Fig. 1E). In addition, high LY6K expression was discovered to predict worse overall survival in patients with OSCC (Fig. 1F). All in all, abnormally high LY6K expression was identified in OSCC, which predicted poorer survival of OSCC patients.

LY6K knockdown inhibited OSCC tumorigenesis and metastasis

The biological function of LY6K in OSCC was evaluated by silencing LY6K in CAL27 and HN4 cells (Fig. 2A,B). The CCK-8 assay indicated that LY6K depletion substantially suppressed the viability of treated cells (Fig. 2C). Similar results were obtained from the colony formation assay, where cells transfected with shLY6K exhibited noticeably inhibited colony formation capacity (Fig. 2D). In addition, we observed that the migrative and invasive abilities of CAL27 and HN4 cells were significantly reduced in the LY6K-knockdown group (Fig. 2E,F). Furthermore, the xenograft tumors developed from LY6K-depleted CAL27 cells were significantly smaller in size and weight than the tumors from the control group (Fig. 2G,H). In a lung metastasis model, mice injected with LY6K shRNA-infected cells exhibited a significantly reduced number of metastatic nodules (Fig. 2I). These data suggest that the growth and metastasis of OSCC could be inhibited by silencing LY6K.

LY6K modulated CAV-1-mediated MAPK/ERK signaling in OSCC

Subsequently, we explored the mechanism underlying the tumor-promoting effect of LY6K by assessing the levels of CAV-1, ERK, and p-ERK in LY6K-silenced OSCC cells. Western blot indicated that CAV-1 and p-ERK levels were substantially suppressed in cells transfected with shLY6K (Fig. 3A). In cells overexpressing LY6K, the expression of LY6K, CAV-1, and p-ERK was dramatically increased (Fig. 3B). However, the introduction of MEK inhibitor (PD98059) or shCAV-1 substantially inhibited the protein level of p-ERK in LY6K-overexpressed OSCC cells (Fig. 3C), indicating that LY6K probably activated ERK signaling via CAV-1. To confirm the interaction between LY6K

and CAV-1, LY6K and CAV-1 expression was found to be positively correlated in OSCC tissues (Fig. 3D). The Co-IP assay indicated that LY6K binds with CAV-1 in OSCC cells (Fig. 3E). These results suggested that LY6K activated ERK signaling by enhancing CAV-1 expression.

LY6K promoted the tumorigenesis of OSCC via CAV-mediated activation of ERK signaling

Next, we investigated the biological role of CAV-1-mediated ERK signaling activation in LY6K-promoted OSCC tumorigenesis. The CCK-8 assay indicated that CAV-1 knockdown or PD98059 treatment could abrogate the promotive effect of LY6K abundance on the viability of OSCC cells (Fig. 4A). Meanwhile, cells transfected with oeLY6K presented enhanced colony formation capacity, which could be attenuated by either CAV-1 deficiency or inhibition of ERK signaling (Fig. 4B). In Transwell assays, LY6K overexpression promoted the migration and invasion of the treated cells but shCAV-1 transfection or PD98059 treatment attenuated this promotion (Fig. 4C,D). Taken together, CAV-1-mediated ERK signaling was

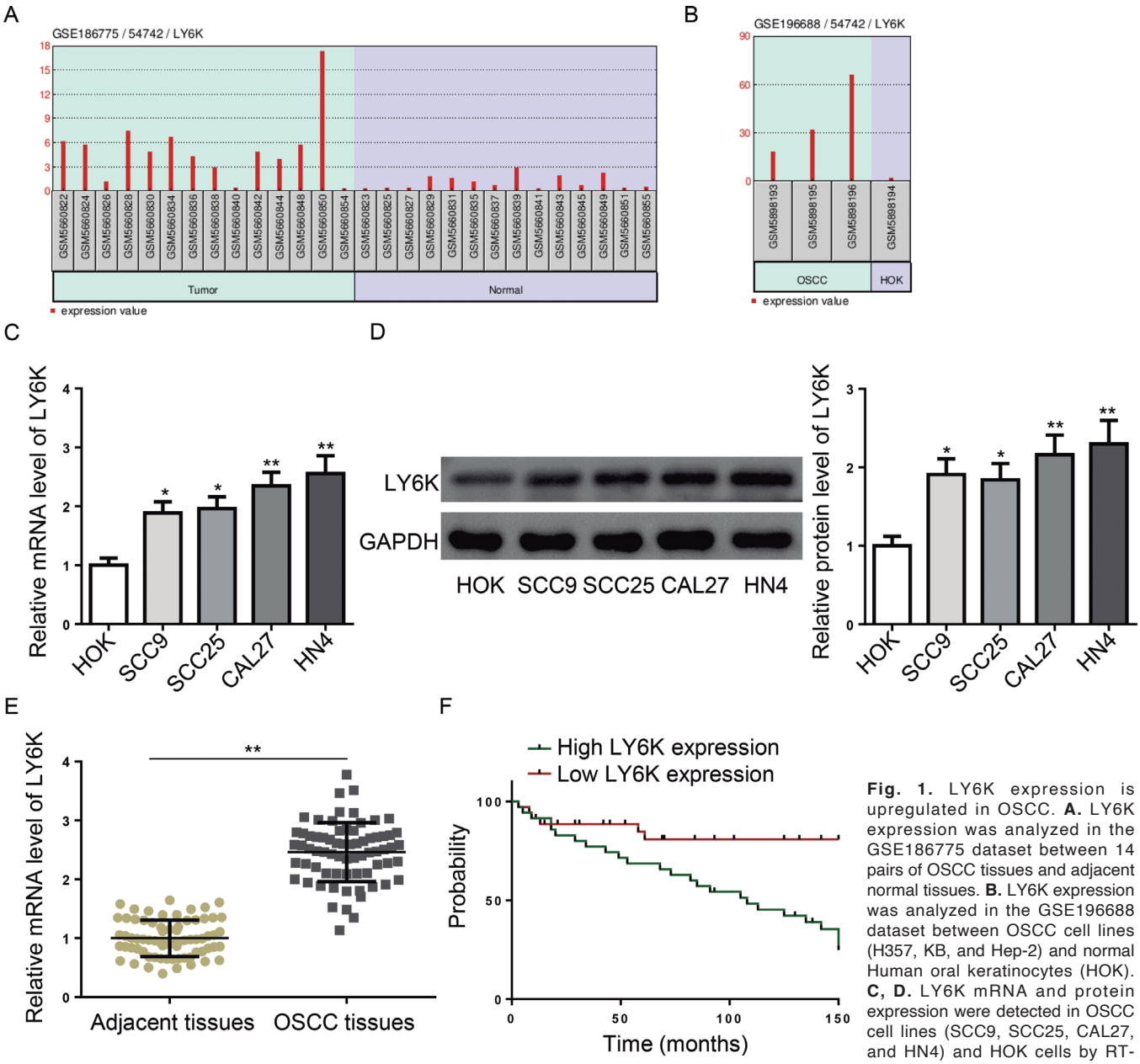

Fig. 1. LY6K expression is upregulated in OSCC. **A.** LY6K expression was analyzed in the GSE186775 dataset between 14 pairs of OSCC tissues and adjacent normal tissues. **B.** LY6K expression was analyzed in the GSE196688 dataset between OSCC cell lines (H357, KB, and Hep-2) and normal Human oral keratinocytes (HOK). **C, D.** LY6K mRNA and protein expression were detected in OSCC cell lines (SCC9, SCC25, CAL27, and HN4) and HOK cells by RT-qPCR and western blot, respectively. **E.** RT-qPCR compared the expression of LY6K between clinically resected tumor and non-tumor tissues. **F.** Kaplan-Meier analysis of the association between LY6K expression and overall survival in OSCC patients. **P*<0.05, ***P*<0.01.

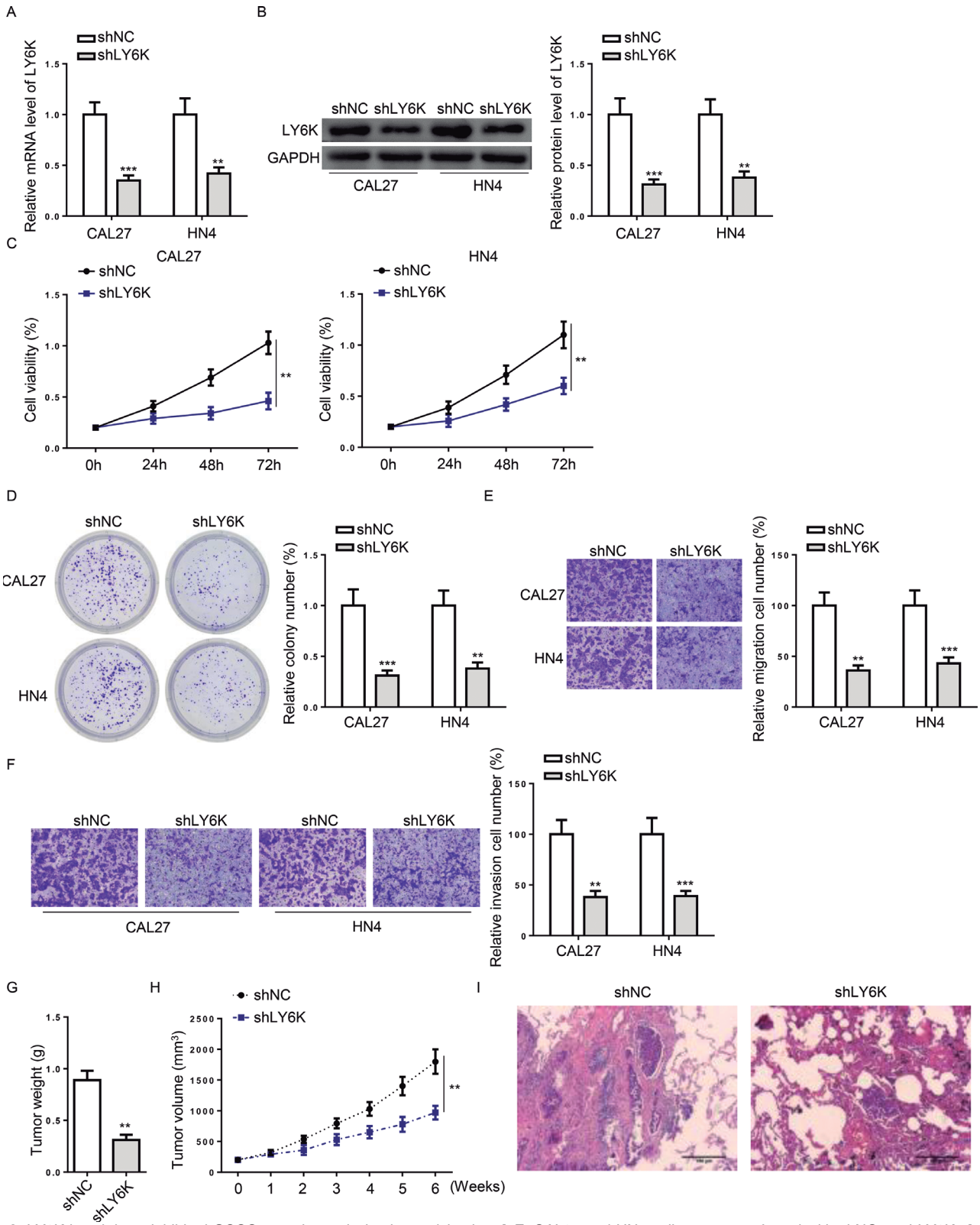

Fig. 2. LY6K knockdown inhibited OSCC tumorigenesis *in vitro* and *in vivo*. **A-F.** CAL27 and HN4 cells were transfected with shNC or shLY6K. **A, B.** The mRNA and protein expression of LY6K was evaluated. **C, D.** The proliferative ability of the cells was assessed using CCK-8 and colony formation assays. **E, F.** Transwell chambers were applied to assess the migration and invasion of treated cells. **G, H.** Weight and volume of the xenograft tumors in control and LY6K-silenced groups. **I.** The metastatic nodules in the mouse model were evaluated using H&E staining. ***P*<0.01, ****P*<0.001.

indispensable for LY6K to facilitate OSCC progression.

FTO induced LY6K upregulation in an m^{6}A-dependent manner

RM2Target predicted that FTO could bind with LY6K and two pieces of perturbation evidence indicated that FTO positively regulated LY6K expression (Fig. 5A,B). Therefore, we measured FTO levels and discovered that FTO was upregulated in OSCC cells and tissues (Fig. 5C-E). Additionally, there was a positive correlation between FTO expression and LY6K expression in OSCC tissues (Fig. 5F). FTO knockdown in CAL27 and HN4 cells decreased LY6K mRNA and protein levels (Fig. 5G,H). To validate whether FTO regulated LY6K expression through m^{6}A modification, MeRIP-qPCR was performed. As presented in Fig. 5I, FTO depletion markedly increased m^{6}A enrichment in LY6K mRNA. Moreover, FTO knockdown only affected the luciferase activity of LY6K-WT but not that of LY6K-Mut (Fig. 5J). Thus, we can summarize that FTO induced LY6K upregulation in OSCC via m^{6}A modification.

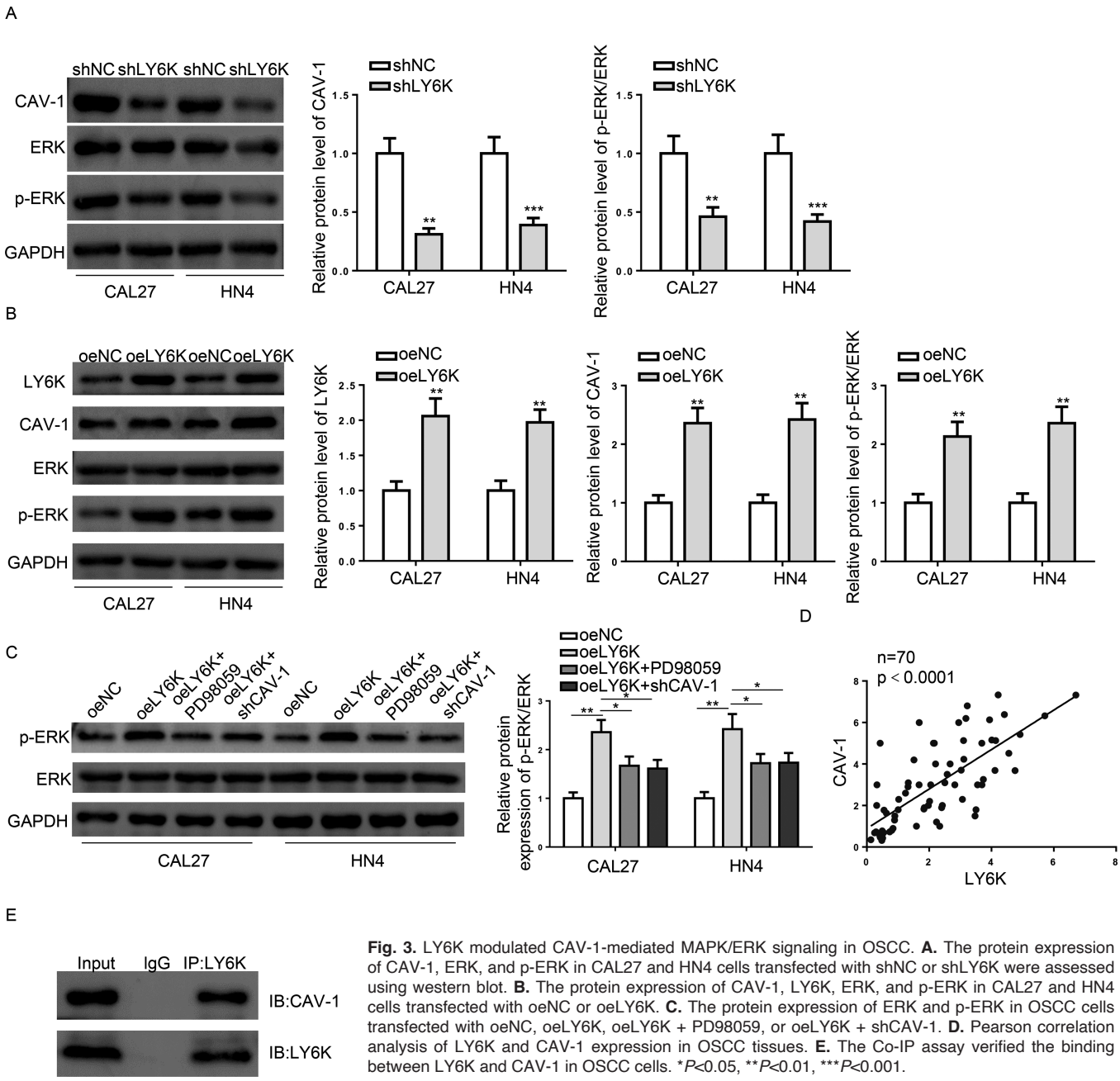

Fig. 3. LY6K modulated CAV-1-mediated MAPK/ERK signaling in OSCC. **A.** The protein expression of CAV-1, ERK, and p-ERK in CAL27 and HN4 cells transfected with shNC or shLY6K were assessed using western blot. **B.** The protein expression of CAV-1, LY6K, ERK, and p-ERK in CAL27 and HN4 cells transfected with oeNC or oeLY6K. **C.** The protein expression of ERK and p-ERK in OSCC cells transfected with oeNC, oeLY6K, oeLY6K + PD98059, or oeLY6K + shCAV-1. **D.** Pearson correlation analysis of LY6K and CAV-1 expression in OSCC tissues. **E.** The Co-IP assay verified the binding between LY6K and CAV-1 in OSCC cells. **P*<0.05, ***P*<0.01, ****P*<0.001.

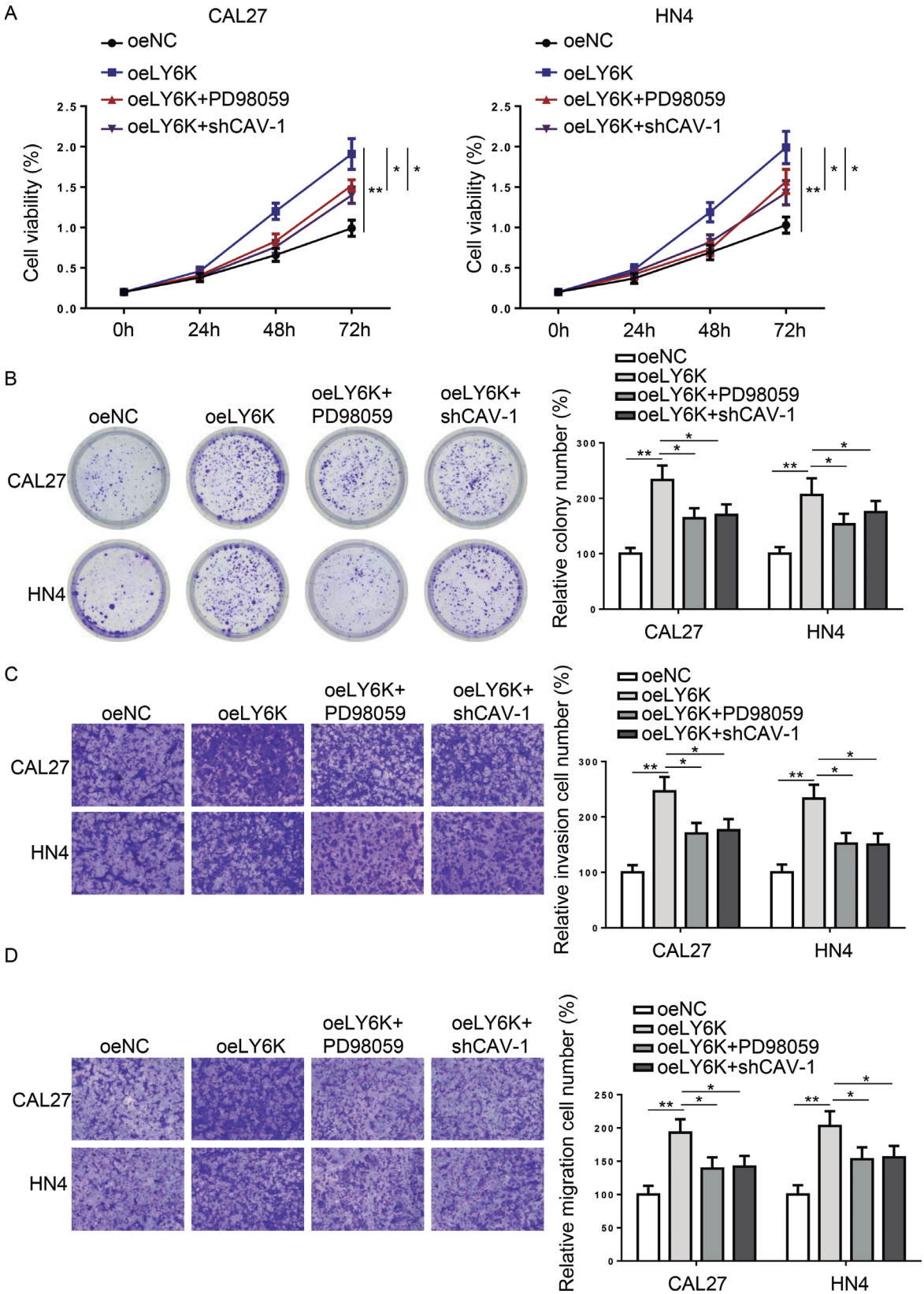

Fig. 4. LY6K promoted the tumorigenesis of OSCC via CAV-mediated activation of ERK signaling. CAL27 and HN4 cells were treated with oeNC, oeLY6K, oeLY6K + shCAV-1, or oeLY6K + PD98059. **A, B.** The proliferation and colony formation capacity were evaluated. **C, D.** Transwell assay determined the migration and invasion of the cells. **P*<0.05, ***P*<0.01.

A

RM2Target ID	WERs Name	WERs Type	Target Gene	Modification	Organism	Cell Line/Tissue	Validated	Binding	Perturbation	Confidence score
RM2Target_718272	FTO	Eraser	LY6K	m6A,m6Am	Homo sapiens	HeLa	-	1/1	-	1
RM2Target_718271	FTO	Eraser	LY6K	m6A,m6Am	Homo sapiens	253J	-	-	1/1	1
RM2Target_718273	FTO	Eraser	LY6K	m6A,m6Am	Homo sapiens	OVCAR5	-	-	1/2	1

B

WER	Analysis ID	PMID	GSE ID	Source (Cell line/Tissue)	Target gene	Log2FC	P-value	Adj.P-value	Perturbation direction	Perturbation effect	Method
FTO	Ana_expr_hsa_20	-	GSE130350	OVCAR5	LY6K	1.0168	0.00034838	0.0027658	OE	up-regulated	RNA-seq

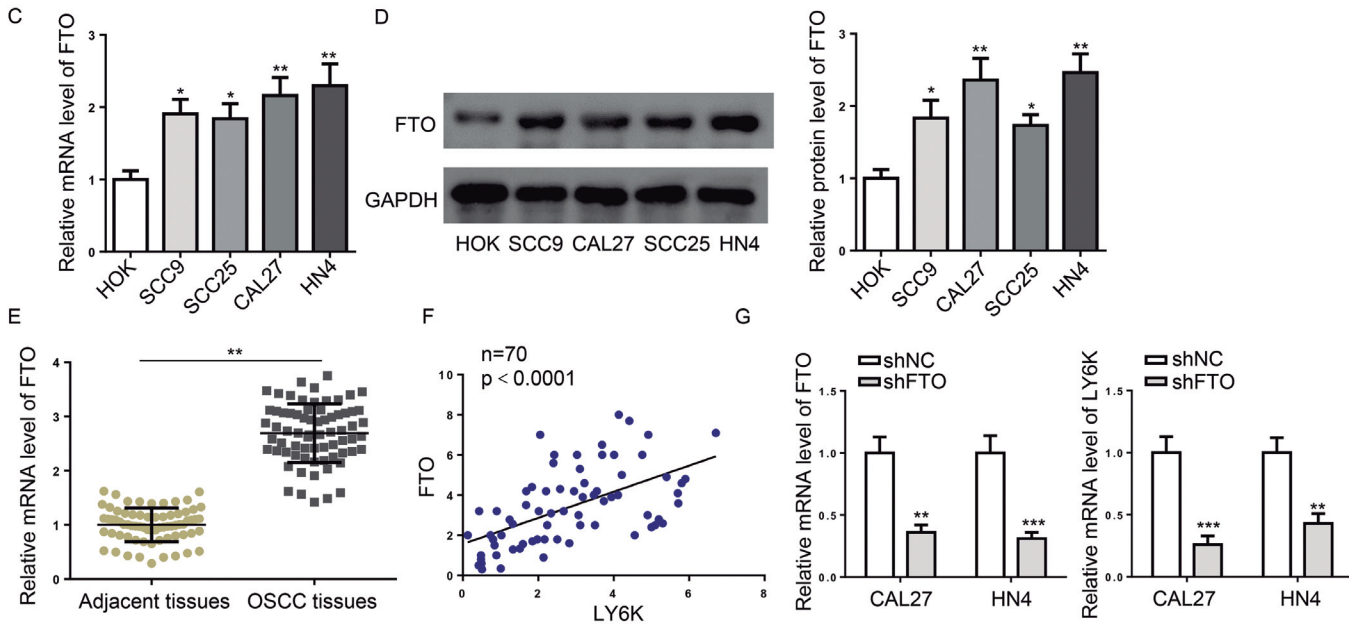

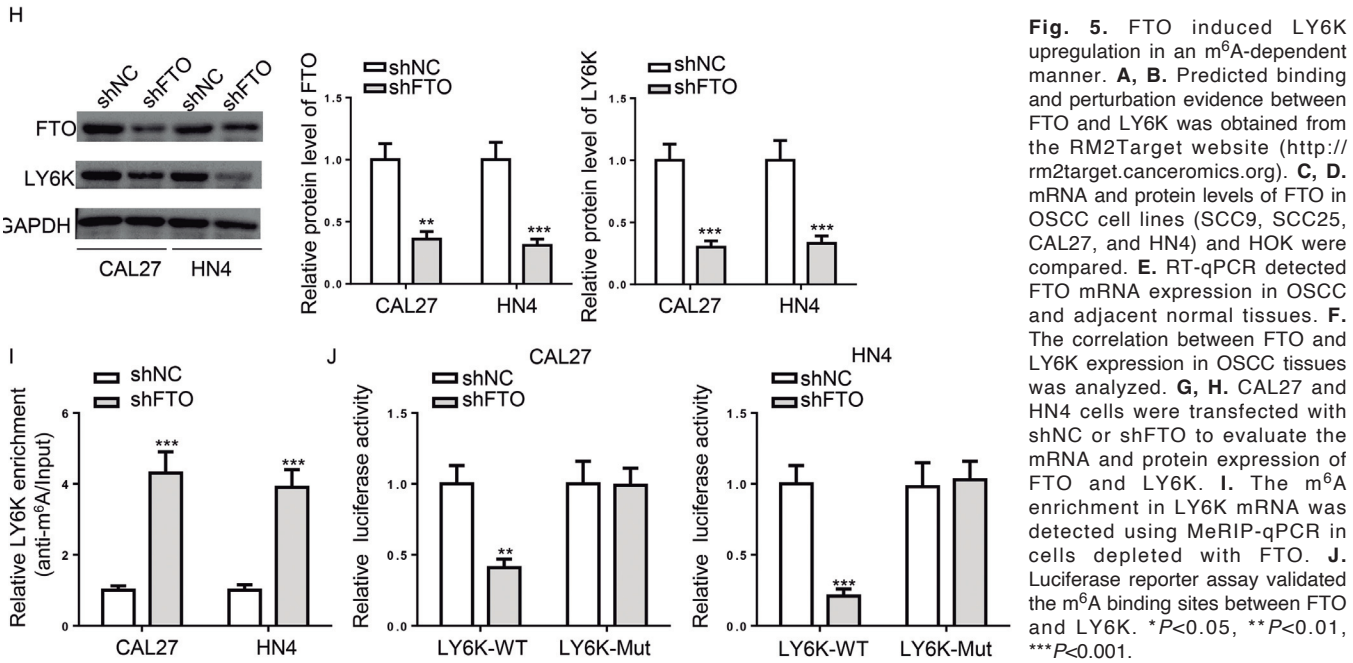

Fig. 5. FTO induced LY6K upregulation in an m^{6}A-dependent manner. **A, B.** Predicted binding and perturbation evidence between FTO and LY6K was obtained from the RM2Target website (http://rm2target.canceromics.org). **C, D.** mRNA and protein levels of FTO in OSCC cell lines (SCC9, SCC25, CAL27, and HN4) and HOK were compared. **E.** RT-qPCR detected FTO mRNA expression in OSCC and adjacent normal tissues. **F.** The correlation between FTO and LY6K expression in OSCC tissues was analyzed. **G, H.** CAL27 and HN4 cells were transfected with shNC or shFTO to evaluate the mRNA and protein expression of FTO and LY6K. **I.** The m^{6}A enrichment in LY6K mRNA was detected using MeRIP-qPCR in cells depleted with FTO. **J.** Luciferase reporter assay validated the m^{6}A binding sites between FTO and LY6K. **P*<0.05, ***P*<0.01, ****P*<0.001.

IGF2BP1 cooperated with FTO to regulate the translation of LY6K

Next, we investigated the m^{6}A reader that cooperates with FTO to promote LY6K translation. RM2Target forecasted potent binding between LY6K and IGF2BP1 (Fig. 6A) and perturbation evidence showed that IGF2BP1 knockdown upregulated LY6K (Fig. 6B). RIP assay indicated that FTO knockdown significantly reduced IGF2BP1 enrichment at LY6K transcripts in OSCC cells (Fig. 6C). Furthermore, IGF2BP1 depletion rescued the decrease in LY6K expression caused by FTO knockdown in CAL27 and HN4 cells (Fig. 6D,E). Additionally, IGF2BP1 depletion abrogated the decrease in stability of LY6K mRNA caused by FTO deficiency (Fig. 6F). Our data imply that FTO cooperated with

A

RM2Target ID	WERs Name	WERs Type	Target Gene	Modification	Organism	Cell Line/Tissue	Validated	Binding	Perturbation	Confidence score
RM2Target_933325	IGF2BP1	Reader	LY6K	m6A	Homo sapiens	A549	-	-	3/3	3
RM2Target_933326	IGF2BP1	Reader	LY6K	m6A	Homo sapiens	K562	-	1/1	-	1
RM2Target_933324	IGF2BP1	Reader	LY6K	m6A	Homo sapiens	SK-N-AS	-	-	1/1	1

B

WER	Analysis ID	PMID	GSE ID	Source (Cell line/Tissue)	Target gene	Log2FC	P-value	Adj.P-value	Perturbation direction	Perturbation effect	Method
IGF2BP1	Ana_expr_hsa_40	32761127	GSE146546	A549	LY6K	1.3252	0.011115	0.036366	KO	up-regulated	RNA-seq
IGF2BP1	Ana_expr_hsa_41	32761127	GSE146547	A549	LY6K	2.8918	0.021594	0	KD	up-regulated	RNA-seq
IGF2BP1	Ana_expr_hsa_60	33829040	GSE161087	A549	LY6K	2.8924	0.013149	0	KD	up-regulated	RNA-seq

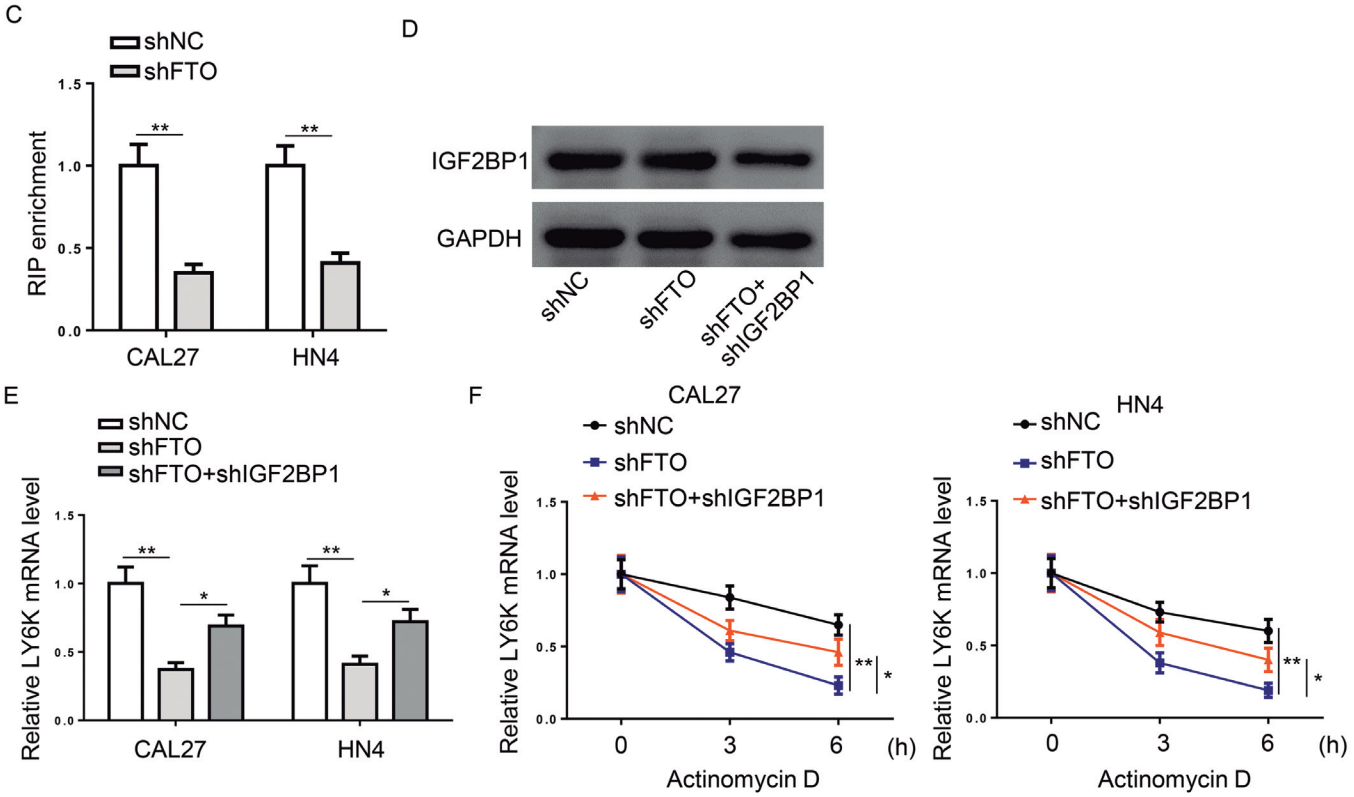

Fig. 6. IGF2BP1 cooperated with FTO to regulate the translation of LY6K. **A, B.** Predicted binding and perturbation evidence between IGF2BP1 and LY6K was obtained from the RM2Target database. **C.** IGF2BP1 was immunoprecipitated and then subjected to qRT-PCR to assess LY6K transcript levels in OSCC cells transfected with shNC or shFTO. **D-F.** OSCC cells were transfected with shNC, shFTO, or shFTO + shIGF2BP1 to assess the protein expression of IGF2BP1 **(D)** and the mRNA expression of LY6K **(E)**, and LY6K mRNA levels after actinomycin D treatment **(F)**. **P*<0.05, ***P*<0.01.

IGF2BP1 to modulate LY6K mRNA levels.

Discussion

As a glycosylphosphatidylinositol (GPI)-anchored protein, LY6K is located at the plasma membrane and affects various cellular functions, including cell differentiation, proliferation, migration, adhesion, and invasion in lung adenocarcinoma, esophageal cell carcinoma, breast cancer, and cervical cancer, among others (Ishikawa et al., 2007; Kong et al., 2016; Benti et al., 2020). The current study is the first report on the expression pattern, biological function, and molecular mechanism of LY6K in OSCC. LY6K expression was aberrantly high in OSCC tissues and cell lines according to both GEO datasets and clinical data. Besides, high LY6K expression was associated with worse survival of patients with OSCC. By silencing LY6K, we observed that LY6K deficiency effectively inhibited the viability and mobility of OSCC cells. Moreover, established *in vivo* models indicated that LY6K depletion could suppress the growth and metastasis of xenograft OSCC tumors.

During cancer development, dysregulation of gene expression often impairs signaling pathways or causes aberrant signal transduction, leading to hallmark features of cancer (Park et al., 2020; Li et al., 2021). The MAPK signaling pathway is one of the most highly dysregulated signaling pathways in OSCC (Cheng et al., 2022). Among the members of the MAPK pathway, MAPK/ERK signaling has been proven to play a tumor-promoting role in OSCC (Degen et al., 2012; Fu and Feng, 2015; Feng et al., 2019). Moreover, accumulating evidence indicated that the activation of MAPK pathways can be mediated by CAV-1 (Guan et al., 2016; Zhang et al., 2019), a primary structural protein of caveolae and a key regulator of cellular signaling (Jiang et al., 2022). In addition, CAV-1 has been identified as a therapeutic biomarker of OSCC (Bau et al., 2011; Jaafari-Ashkavandi and Aslani, 2017; Kaya et al., 2021). Considering that LY6K was proven to bind with CAV-1 and mediate ERK signaling in cancer, we hypothesized that LY6K binds with CAV-1, resulting in the activation of MAPK/ERK signaling in OSCC, which was verified by our laboratory data. Furthermore, functional assays suggested that CAV-1 knockdown or inhibition of ERK signaling could attenuate the tumor-promoting effect of LY6K abundance, indicating that the CAV-1-mediated MAPK/ERK activation was indispensable for LY6K-regulated OSCC progression.

Mounting studies have demonstrated that m^6A modification could affect the destiny of modified RNA molecules and, therefore, interfere with cancer development (An and Duan, 2022). Moreover, the significant function of dysregulated m^6A modification regulators has been reported in OSCC (Huang et al., 2020; Liu et al., 2020). Using the online RM2Target database, FTO was identified to target LY6K and positively regulate LY6K expression in cancer cell lines. Besides, the m^6A reader IGF2BP1 was predicted to bind with LY6K. The cooperation between FTO and IGF2BP1 has been reported in cancers. Wang et al. (2021) uncovered that FTO cooperated with IGF2BP1 to downregulate DACT1 via m^6A demethylation, therefore activating Wnt signaling to promote osteosarcoma progression (Lv et al., 2022). Xie et al. revealed that inhibition of FTO recruited IGF2BP1 to increase the mRNA stability of SOCS1 and subsequently activate p53 signaling to exert anti-cancer effects in breast cancer (Xie et al., 2022). In OSCC, FTO has been proven to exert tumor-promoting effects by regulating m^6A modification of its downstream genes with the help of m^6A readers. For example, FTO knockdown inhibited OSCC tumorigenesis by degradation of YAP1 mRNA by increasing its m^6A modification following YTHDF2 reading and recognition (Li et al., 2022). FTO depletion activated autophagy to retard the malignant development of OSCC by facilitating YTHDF2 to degrade eIF4G1 mRNA (Wang et al., 2021). In our study, it was proven that FTO facilitated the progression of oncogene LY6K in OSCC by mediating IGF2BP1-dependent m^6A modification.

Collectively, this investigation uncovered that LY6K served as an oncogene in OSCC and the stable knockdown of LY6K could suppress the tumorigenesis and metastasis of OSCC. Mechanically, LY6K triggered CAV-1-mediated MAPK/ERK signaling activation, while upregulation in OSCC was induced by FTO-mediated m^6A demethylation, which was recognized and stabilized by IGF2BP1. These findings offer novel insights into the molecular mechanisms of OSCC tumorigenesis and metastasis, which may help to improve the diagnosis and treatment of patients with OSCC.

Funding. This work was funded by the Changzhou Municipal Health Commission Youth Project (QN201936), the Research of Preparation and Properties of Ultra-high Molecular Weight Polyethylene Fiber Ceramic Matrix Composite Resin Material (WZ202112), and the 2023 Changzhou Health Talents Domestic Research and Training Funding Project (GN2023012).

References

An Y and Duan H. (2022). The role of m^6A RNA methylation in cancer metabolism. Mol. Cancer 21, 1, 14.

Arellano-Garcia M.E., Li R., Liu X., Xie Y., Yan X., Loo J.A. and Hu S. (2010). Identification of tetranectin as a potential biomarker for metastatic oral cancer. Int. J. Mol. Sci. 11, 9, 3106-3121.

Bau D.T., Tsai M.H., Tsou Y.A., Wang C.H., Tsai C.W., Sun S.S., Hua C.H., Shyue S.K. and Tsai R.Y. (2011). The association of Caveolin-1 genotypes with oral cancer susceptibility in Taiwan. Ann. Surg. Oncol. 18, 5, 1431-1438.

Benti S., Tiwari P.B., Goodlett D.W., Daneshian L., Kern G.B., Smith M.D., Uren A., Chruszcz M., Shimizu L.S. and Upadhyay G. (2020). Small molecule binds with lymphocyte antigen 6K to induce cancer Cell Death 12, 509.

Caballero O.L. and Chen Y.-T. (2012). Cancer/testis antigens: Potential targets for immunotherapy. In: Innate immune regulation and cancer immunotherapy. Wang R. (ed). Springer New York, New York, NY. pp 347-369.

Carrero I., Liu H.C., Sikora A.G., and Milosavljevic A. (2019). Histoepigenetic analysis of HPV- and tobacco-associated head and neck cancer identifies both subtype-specific and common therapeutic targets despite divergent microenvironments. Oncogene 38, 19, 3551-3568.

Cheng Y., Chen J., Shi Y., Fang X. and Tang Z. (2022). MAPK signaling pathway in oral squamous Cell Carcinoma: Biological function and targeted therapy. Cancers 14, 4625.

de Nooij-van Dalen A.G., van Dongen G.A., Smeets S.J., Nieuwenhuis E.J.C., Walsum M.S.V., Snow G.B. and Brakenhoff R.H. (2003). Characterization of the human Ly-6 antigens, the newly annotated member Ly-6K included, as molecular markers for head-and-neck squamous cell carcinoma. Int. J. Cancer 103, 6, 768-774.

Degen M., Natarajan E., Barron P., Widlund H.R. and Rheinwald J.G. (2012). MAPK/ERK-Dependent translation factor hyperactivation and dysregulated laminin γ2 expression in oral dysplasia and squamous cell carcinoma. Am. J. Pathol. 180, 2462-2478.

Feng J., Xu J., Xu Y., Xiong J., Xiao T., Jiang C., Li X., Wang Q., Li J. and Li Y. (2019). CLIC1 promotes the progression of oral squamous cell carcinoma via integrins/ERK pathways. Am. J. Transl. Res. 11, 557-571.

Fu X. and Feng Y. (2015). QKI-5 suppresses cyclin D1 expression and proliferation of oral squamous cell carcinoma cells via MAPK signalling pathway. Int. J. Oral Maxillofac. Surg. 44, 562-567.

Fujihara Y., Miyata H. and Ikawa M. (2018). Factors controlling sperm migration through the oviduct revealed by gene-modified mouse models. Exp. Anim. 67, 91-104.

Guan X., Wang N., Cui F., Liu Y., Liu P., Zhao J., Han C., Li X., Leng Z., Li Y., Ji X., Zou W. and Liu J. (2016). Caveolin-1 is essential in the differentiation of human adipose-derived stem cells into hepatocyte-like cells via an MAPK pathway-dependent mechanism. Mol. Med. Rep. 13, 1487-1494.

Huang G.Z., Wu Q.Q., Zheng Z.N., Shao T.R., Chen Y.C., Zeng W.S. and Lv X.Z. (2020). M^6A-related bioinformatics analysis reveals that HNRNPC facilitates progression of OSCC via EMT. Aging 12, 11667-11684.

Ishikawa N., Takano A., Yasui W., Inai K., Nishimura H., Ito H., Miyagi Y., Nakayama H., Fujita M., Hosokawa M., Tsuchiya E., Kohno N., Nakamura Y. and Daigo Y. (2007). Cancer-testis antigen lymphocyte antigen 6 complex locus K is a serologic biomarker and a therapeutic target for lung and esophageal carcinomas. Cancer Res. 67, 11601-11611.

Jaafari-Ashkavandi Z. and Aslani E. (2017). Caveolin-1 expression in oral lichen planus, dysplastic lesions and squamous cell carcinoma. Pathol. Res. Pract. 213, 809-814.

Jiang Y., Krantz S., Qin X., Li S., Gunasekara H., Kim Y.M., Zimnicka A., Bae M., Ma K., Toth P.T., Hu Y., Shajahan-Haq A.N., Patel H.H., Gentile S., Bonini M.G., Rehman J., Liu Y. and Minshall R.D. (2022). Caveolin-1 controls mitochondrial damage and ROS production by regulating fission - fusion dynamics and mitophagy. Redox Biol. 52, 102304.

Kaya S., Wiesmann N., Goldschmitt J., Krüger M., Al-Nawas B. and Heider J. (2021). Differences in the expression of caveolin-1 isoforms in cancer-associated and normal fibroblasts of patients with oral squamous cell carcinoma. Clin. Oral Investig. 25, 5823-5831.

Keinänen A., Uittamo J., Marinescu-Gava M., Kainulainen S. and Snäll J. (2021). Preoperative C-reactive protein to albumin ratio and oral health in oral squamous cell carcinoma patients. BMC Oral Health 21, 132.

Kim Y.S., Park S.J., Lee Y.S., Kong H.K. and Park J.H. (2016). miRNAs involved in LY6K and estrogen receptor α contribute to tamoxifen-susceptibility in breast cancer. Oncotarget 7, 42261-42273.

Kong H., Park S., Kim Y. and Park J.H. (2014). Epigenetic modification of LY6K in CGI shore and CGI regulates LY6K gene activation and metastatic function in breast cancer. Cancer Res. 74, 1365-1365.

Kong H.K., Park S.J., Kim Y.S., Kim K.M., Lee H.W., Kang H.G., Woo Y.M., Park E.Y., Ko J.Y., Suzuki H., Chun K.H., Song E., Jang K.Y. and Park J.H. (2016). Epigenetic activation of LY6K predicts the presence of metastasis and poor prognosis in breast carcinoma. Oncotarget 7, 55677-55689.

Kono K., Mizukami Y., Daigo Y., Takano A., Masuda K., Yoshida K., Tsunoda T., Kawaguchi Y., Nakamura Y. and Fujii H. (2009). Vaccination with multiple peptides derived from novel cancer-testis antigens can induce specific T-cell responses and clinical responses in advanced esophageal cancer. Cancer Sci. 100, 1502-1509.

Li X., Zhang B., Yu K., Bao Z., Zhang W. and Bai Y. (2021). Identifying cancer specific signaling pathways based on the dysregulation between genes. Comput. Biol. Chem. 95, 107586.

Li D.Q., Huang C.C., Zhang G. and Zhou L.L. (2022). FTO demethylates YAP mRNA promoting oral squamous cell carcinoma tumorigenesis. Neoplasma 69, 71-79.

Liu L., Wu Y., Li Q., Liang J., He Q., Zhao L., Chen J., Cheng M., Huang Z., Ren H., Chen J., Peng L., Gao F., Chen D. and Wang A. (2020). METTL3 promotes tumorigenesis and metastasis through BMI1 m6A methylation in oral squamous cell carcinoma. Mol. Ther. 28, 2177-2190.

Lv D., Ding S., Zhong L., Tu J., Li H., Yao H., Zou Y., Zeng Z., Liao Y., Wan X., Wen L. and Xie X. (2022). M6A demethylase FTO-mediated downregulation of DACT1 mRNA stability promotes Wnt signaling to facilitate osteosarcoma progression. Oncogene 41, 1727-1741.

Park J.H., Pyun W.Y. and Park H.W. (2020). Cancer metabolism: Phenotype, signaling and therapeutic targets. Cells 9, 2308.

Park S., Park D.; Han S., Chung G.E., Soh S., Ka H.I., Joo H.J. and Yang Y. (2023). LY6K depletion modulates TGF-β and EGF signaling. 12, 12593-12607.

Sastry N.G., Wan X., Huang T., Alvarez A.A., Pangeni R.P., Song X., James C.D., Horbinski C.M., Brennan C.W., Nakano I., Hu B. and Chen S.Y. (2020). LY6K promotes glioblastoma tumorigenicity via CAV-1-mediated ERK1/2 signaling enhancement. Neuro-Oncol. 22, 1315-1326.

Vitório J.G., Duarte-Andrade F.F., Pereira T.D.S.F., Fonseca F.P., Amorim L.S.D., Martin-Chaves R.R., Gomes C.C., Canuto G.A.B. and Gomez R.S. (2020). Metabolic landscape of oral squamous cell carcinoma. Metabolomics 16, 105.

Wang F., Liao Y., Zhang M., Zhu Y., Wang W., Cai H., Liang J., Song F., Hou C., Huang S., Zhang Y., Wang C. and Hou J. (2021). N^6-methyladenosine demethyltransferase FTO-mediated autophagy in malignant development of oral squamous cell carcinoma. Oncogene 40, 3885-3898.

Wang R. and Wang Y. (2021). Fourier transform infrared spectroscopy in oral cancer diagnosis. Int. J. Mol. Sci. 22, 1206.

Xie G., Wu X.N., Ling Y., Rui Y., Wu D., Zhou J., Li J., Lin S., Peng Q., Li Z., Wang H. and Luo H.B. (2022). A novel inhibitor of N6 -

methyladenosine demethylase FTO induces mRNA methylation and shows anti-cancer activities. Acta Pharm. Sin. B 12, 853-866.

Yang C.M., Chang H.S., Chen H.C., You J.J., Liou H.H., Ting S.C., Ger L.P., Li S.C. and Tsai K.W. (2019). Low C6orf141 expression is significantly associated with a poor prognosis in patients with oral cancer. Sci. Rep. 9, 4520.

Zhang C., Wu Q., Huang H., Chen X., Huang T., Li W., Liu Y. and Zhang J. (2019). Caveolin-1 promotes Rfng expression via Erk-Jnk-p38 signaling pathway in mouse hepatocarcinoma cells. J. Pysiol. Biochem. 75, 549-559.

Accepted February 27, 2024